Optimization of highly nonlinear dispersion-flattened photonic crystal fiber for supercontinuum generation*

Zhang Ya-Ni(张亚妮)†

Department of Physics and Information Technology, Baoji University of Arts & Science, Baoji 721007, *China*
The Faculty of Advanced Technology, University of Glamorgan, Pontypridd, CF37 1RP, UK

(Received 30 May 2012; revised manuscript received 13 July 2012)

A simple type of photonic crystal fiber (PCF) for supercontinuum generation is proposed for the first time. The proposed PCF is composed of a solid silica core and a cladding with square lattice uniform elliptical air holes, which offers not only a large nonlinear coefficient but also a high birefringence and low leakage losses. The PCF with nonlinear coefficient as large as 46 $W^{-1} \cdot km^{-1}$ at the wavelength of 1.55 μm and a total dispersion as low as ± 2.5 ps $\cdot$ nm$^{-1} \cdot$ km^{-1} over an ultra-broad waveband range of the S–C–L band (wavelength from 1.46 μm to 1.625 μm) is optimized by adjusting its structure parameter, such as the lattice constant Λ, the air-filling fraction f, and the air-hole ellipticity η. The novel PCF with ultra-flattened dispersion, highly nonlinear coefficient, and nearly zero negative dispersion slope will offer a possibility of efficient super-continuum generation in telecommunication windows using a few ps pulses.

Keywords: fiber optics and waveguides, full vector finite element method, confinement loss

PACS: 42.81.–i, 02.70.Dh, 42.81.Gs, 42.90.+m **DOI:** 10.1088/1674-1056/22/1/014214

1. Introduction

Index-guiding photonic crystal fibers (PCFs),[1] also called holey fibers or microstructured optical fibers, are usually formed by a central solid defect region surrounded by multiple air holes with the same diameter arrayed in a regular triangular lattice. The chromatic dispersion profile can be easily controlled by varying the hole diameter and the hole-to-hole spacing.[2] The controllability of chromatic dispersion in a PCF is very important for practical applications to optical communication systems, dispersion compensation, and nonlinear optics.[3] So far, various PCFs with remarkable dispersion properties, for example, zero dispersion wavelengths shifted to the visible and near-infrared wavelengths and an ultra-flattened chromatic dispersion,[4,5] have been reported. However, by using a PCF with hexangular lattice structure uniform air holes in the cladding region, it is difficult to control both the dispersion and the dispersion slope in a wide wavelength range and to obtain a highly nonlinear dispersion flattened PCF (HNDF-PCF) in the 1.55 μm wavelength range. While, the HNDF-PCF has various important applications in nonlinear devices such as an optical parametric oscillator (OPO),[6] optical parametric amplifier (OPA),[7] multi-wavelength lasers,[8,9] and a signal switcher.[10]

To achieve a highly nonlinear coefficient and a nearly-zero ultra-flattened chromatic dispersion in a PCF, several intriguing designs have been proposed.[4] Among them are the the conventional PCF designs with non-uniform optimized air holes,[11,12] a PCF with two-defected air-hole rings,[13] and a nonlinear PCF with several kinds of air-hole diameters.[14] This kind of design has a higher request for fabrication. Thus, the design of a simple PCF structure with highly nonlinear ultra-flattened chromatic dispersion characteristics and low confinement losses is an ongoing challenge.

In this paper, using a simple design technique to change the cladding hexangular lattice structure to a square lattice structure, and by changing the cladding circle air holes to elliptical air holes, we obtain a simple structure HNDF-PCF, which is composed of a solid silica core and a cladding with square lattice uniform elliptical air holes along the fiber length. Note that the proposed HNDF-PCF will be very easy to fabricate by adopting capillary stacking technology.[15] The numerical research is processed by using the full-vector finite element method (FV-FEM),[16] and the results show that the proposed HNDF-PCF will present a highly nonlinear coefficient, a small normal group-velocity dispersion, a high birefringence, and low leakage losses. This innovation HNDF-PCF with a total ultra-flattened dispersion as low as ± 2.5 ps $\cdot$ nm$^{-1} \cdot$ km^{-1} over an ultra-broad waveband range of the S–C–L band, a nonlinear coefficient as large as 46 $W^{-1} \cdot km^{-1}$, a confinement leakage loss as low as 0.016 dB $\cdot$ km^{-1}, and a birefringence as high as 3.2×10^{-3} at the wavelength of 1.55 μm is optimized further by adjusting its structure parameter, such as the lattice constant Λ, the air-filling fraction f, and the air-hole ellipticity η. Thus,

*Project supported by the China Scholarship Council Western Talent Project, China (Grant No. 20095004), the Key Science and Technology Program of Shaanxi Province, China (Grant No. 2010K01-078), the Natural Science Foundation of the Education Department of Shaanxi Province, China (Grant No. 2010JK403), the Science and Technology Program of Baoji, China (Grant No. 2010BJ02), and the Key Program of Scientific Research of Baoji College of Arts and Science, China (Grant No. ZK11016).

†Corresponding author. E-mail: yanizhang1@163.com

© 2013 Chinese Physical Society and IOP Publishing Ltd

the proposed HNDF-PCF is very suitable for efficient supercontinuum (SC) generation in the telecommunication window.

2. Design principle of the HNDF-PCF

The cross section of the proposed HNDF-PCF is depicted in Fig. 1. The whole fiber is based on pure silica. The air holes are arranged in a square lattice structure along the fiber length, and the central air hole is eliminated to form a light propagation region. All cladding air holes are uniformly squeezed in the y axis direction to form elliptical air holes. This is characterized by the lattice constant Λ, air-filling fraction $f = d/\Lambda$, elliptical air-hole major axis d and minor axis b. Here, we introduce an air-hole ellipticity η to describe the squeezing degree of the PCF. It is defined as $\eta = b/d$. To accurately simulate the proposed PCF architecture, we adopt the FV-FEM[16] with anisotropic perfectly matched layers (PML) to study all the propagation characteristics of the waveguide with high accuracy.

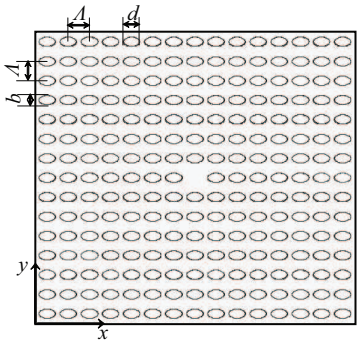


Fig. 1. Schematic cross-section diagram of the proposed HNDF-PCF.

From Maxwell's equations, the basic equation for the FEM can be expressed as

$$\nabla \times ([\mu_r]^{-1} \nabla \times \boldsymbol{E}) - k_0^2 [\varepsilon_r] \boldsymbol{E} = 0, \tag{1}$$

where $\boldsymbol{E}$ denotes the electric field, and $[\varepsilon_r]$ and $[\mu_r]$ are the relative dielectric permittivity and magnetic permeability tensors, respectively.

When the FV-FEM is applied to the PCF, a curvilinear hybrid edge/nodal element[17] is very useful for avoiding spurious solutions and accurately modeling curved boundaries of air holes. Meanwhile, to ensure a high accuracy in reconstructing the structure of the PCF, we use as many as 2^{16} curvilinear hybrid edge/nodal elements for the fiber cross section. Dividing the fiber cross section into 2^{16} curvilinear hybrid elements, from Eq. (1), we can obtain the following eigenvalue equation:

$$[\boldsymbol{K}]\{\boldsymbol{E}\} = k_0^2 n_{\text{eff}}^2 [M]\{\boldsymbol{E}\}, \tag{2}$$

where $[\boldsymbol{K}]$ and $[M]$ are the finite element matrices, and $\{\boldsymbol{E}\}$ is the discrete electric field vector composed of the edge and nodal variables. Utilizing the sparse features of $[\boldsymbol{K}]$ and $[M]$, we solve Eq. (2) using the multi-frontal method, and the effective refractive index of the fundamental mode n_{eff} is obtained.

As we know, the waveguide dispersion $D_{\text{w}}(\lambda)$ of the PCF, depending on n_{eff}, can be determined according to the following formula:[18]

$$D_w(\lambda) = -\frac{\lambda}{c} \frac{\partial^2 |\text{Re}(n_{\text{eff}})|}{\partial \lambda^2}, \tag{3}$$

where c is the velocity of light in a vacuum, Re denotes the real part, and Im denotes the imaginary part. The leakage loss $L_{\text{c}}(\lambda)$ of the PCF, also depending on n_{eff}, can be determined according to the following formula:[19]

$$L_{\text{c}}(\lambda) = \frac{2 \times 10^7}{\ln(10)} \frac{2\pi}{\lambda} \text{Im}[n_{\text{eff}}]. \tag{4}$$

Meanwhile, the nonlinearity coefficient $\gamma(\lambda)$ of the PCF can be defined as[20]

$$\gamma(\lambda) = \frac{2\pi n_2}{\lambda A_{\text{eff}}}, \tag{5}$$

where $n_2 = 3.0 \times 10^{-20}$ m$^2 \cdot$W^{-1} is the nonlinear refractive index of silica, and $A_{\text{eff}}(\lambda)$ is the effective mode area, which is calculated by[21]

$$A_{\text{eff}}(\lambda) = \frac{\left(\iint |\boldsymbol{E}^2| \, \text{d}x\text{d}y\right)^2}{\iint |\boldsymbol{E}|^4 \, \text{d}x\text{d}y}. \tag{6}$$

In the following, we numerically investigate the dependences of dispersion $D_{\text{w}}(\lambda)$ and nonlinearity coefficient $\gamma(\lambda)$ of the proposed PCF on its structural parameters in detail, with the purpose of controlling its dispersion profile and nonlinearity coefficient in a wide wavelength range.

3. Numerical results and discussion

Our design has focused on the total dispersion $D(\lambda)$ in a PCF, which can be approximated using the following relationship:[18]

$$D(\lambda) = D_{\text{w}}(\lambda) + D_{\text{m}}(\lambda), \tag{7}$$

where $D_{\text{m}}(\lambda)$ is the material dispersion and can be obtained using Sellmeier's equation. In order to obtain an ultra-flat dispersion, from Eq. (7), we can see that the PCF can be designed in such a way that the waveguide dispersion is nearly opposite to the material dispersion over a finite range of frequencies.[4] For the PCF, it is very easy to tune $D_{\text{w}}(\lambda)$ by artificially changing the photonic crystal cladding parameters.

3.1. Nonlinearity coefficient and waveguide dispersion analysis of the proposed HNDF-PCF

Firstly, the dependences of $D_{\text{w}}(\lambda)$ and nonlinearity coefficient $\gamma(\lambda)$ on hole pitch Λ are simulated and shown in Fig. 2, by fixing the air-filling fraction $f = 0.6$ and hole ellipticity $\eta = 0.8$ while changing Λ from 1.2 μm to 1.8 μm

with a step of 0.2 μm. It can be seen from Fig. 2(a) that the proposed HNDF-PCF has a negative dispersion parameter and a negative dispersion slope in the wavelength range around 1.55 μm, which demonstrate the excellent dispersion compensating property. The value of $D_{\rm w}(\lambda)$ decreases gradually with the increasing wavelength, Meanwhile, $D_{\rm w}(\lambda)$ is enhanced by changing Λ from 1.2 μm to 1.8 μm. Hence, the minimum dispersion wavelength has a red shift with the increase of Λ . Figure 2(b) shows that $\gamma(\lambda)$ is decreased monotonically with the increase of wavelength, and $\gamma(\lambda)$ shows a gently dipping trend when Λ is increased. It is natural that $\gamma(\lambda)$ is smaller at the wavelength of 1.55 μm when Λ is 1.2 μm. In order to obtain a larger $\gamma(\lambda)$ and through an overall consideration of the dispersion compensating, here, $\Lambda = 1.6$ μm is selected.

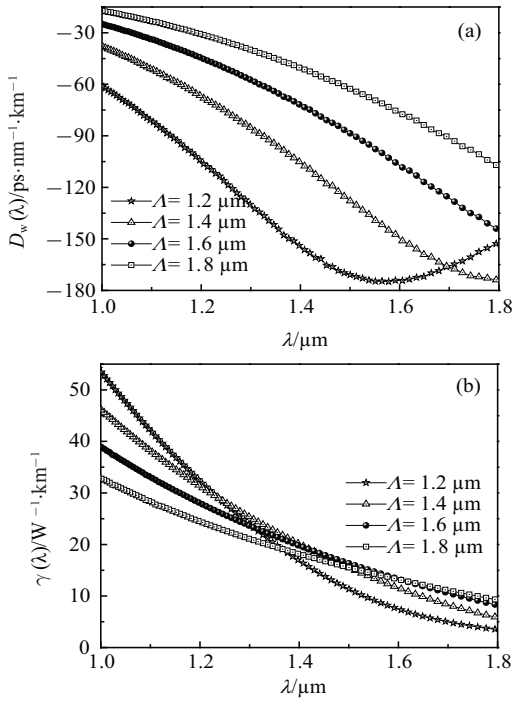


Fig. 2. (a) Waveguide dispersion $D_{\rm w}(\lambda)$ and (b) nonlinearity coefficient $\gamma(\lambda)$ versus wavelength for the proposed HNDF-PCF with different values of pitch Λ. Here, $f = 0.6$ and $\eta = 0.8$.

Next, we fix $\Lambda = 1.6$ μm and $\eta = 0.8$ while changing the air-filling fraction f, the dependences of $D_{\rm w}(\lambda)$ and $\gamma(\lambda)$ on wavelength are depicted in Fig. 3. We can clearly obtain from Fig. 3(a) that the value of negative dispersion increases with the increase of f and wavelength. Figure 3(b) shows that the nonlinearity coefficient curves are almost parallel to each other. When the air-filling fraction f is enlarged, the curve of $\gamma(\lambda)$ is up-shift and the value of $\gamma(\lambda)$ is increased. Here, in order to gain a larger nonlinearity coefficient in the wavelength range around 1.55 μm, the air-filling fraction f must be adjusted to 0.8.

Finally, fixing $f = 0.8$ and $\Lambda = 1.6$ μm while changing air-hole ellipticity η, we analyze the dependences of $D_{\rm w}(\lambda)$ and $\gamma(\lambda)$ on wavelength, and the results are depicted in Fig. 4. It is clearly seen from Fig. 4(a) that the dispersion curve up-shifts with the increase of η, the bigger the value of η is, the more the dispersion curve up-shifts. Figure 4(b) tells us that the value of $\gamma(\lambda)$ will become larger with the increase of η. Here, with the purpose of achieving a larger nonlinearity coefficient and optimizing the dispersion compensation, we fix $\eta = 0.8$ for the proposed HNDF-PCF.

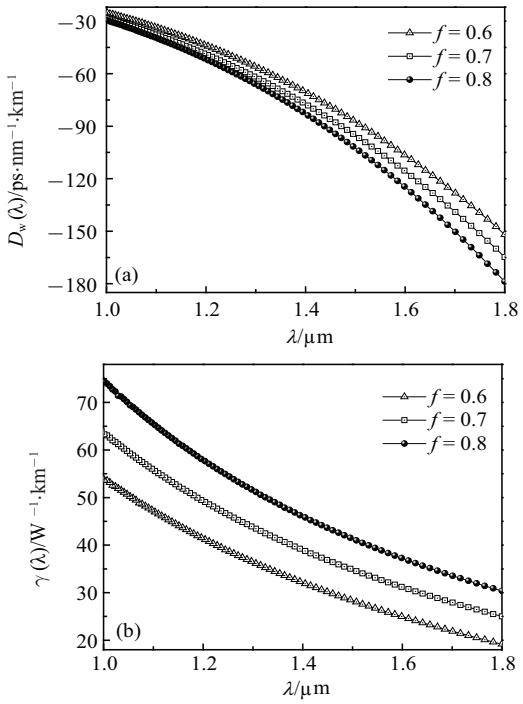


Fig. 3. (a) Waveguide dispersion $D_{\rm w}(\lambda)$ and (b) nonlinearity coefficient $\gamma(\lambda)$ versus wavelength for the proposed HNDF-PCF with different values of f. Here, $\eta = 0.8$ and $\Lambda = 1.6$ μm.

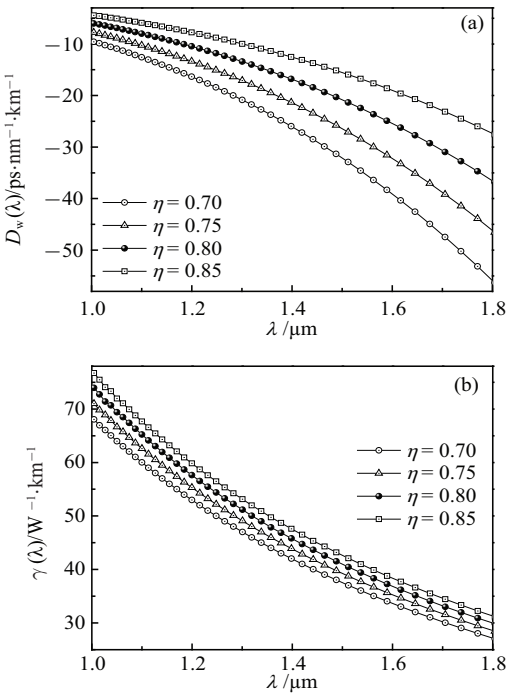


Fig. 4. (a) Waveguide dispersion $D_{\rm w}(\lambda)$ and (b) nonlinearity coefficient $\gamma(\lambda)$ versus wavelength for the proposed HNDF-PCF with different values of η. Here $f = 0.8$ and $\Lambda = 1.6$ μm.

According to the aforementioned discussion, in order to obtain a greater nonlinearity coefficient $\gamma(\lambda)$ and a lower ultra-flattened dispersion in the wavelength range around 1.55 μm, the optimization structure parameters for the proposed square lattice elliptical air-holes PCF are $f = 0.8$, $\eta = 0.8$, and $\Lambda = 1.6$ μm.

3.2. Characteristics of the optimized HNDF-PCF

The total dispersion can be easily calculated based on Eq. (7) for the optimized HNDF-PCF, as shown in Fig. 5(a), and the waveguide and the material dispersion curves have been included in Fig. 5(a). Obviously, the material dispersion, which is a monotonically increasing smooth function of the wavelength, is anti-symmetric with the waveguide dispersion. So, the total dispersion is ultra-flattened within $\pm 2.5\ \mathrm{ps\cdot nm^{-1}\cdot km^{-1}}$ over an ultra broad waveband range of the S–C–L band, as shown in Fig. 5(b), and is nearly zero at the wavelength of 1.54 μm, which is similar to the dispersion parameter of a commercial high nonlinear PCF.[22]

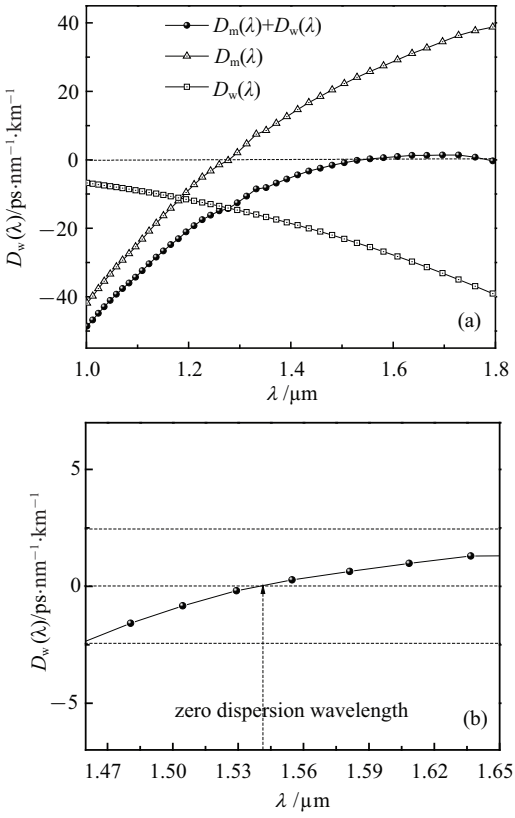


Fig. 5. (a) Waveguide and material dispersions, which lead to a nearly-zero total dispersion; (b) ultra-flattened dispersion within $\pm 2.5\ \mathrm{ps\cdot nm^{-1}\cdot km^{-1}}$ over the waveband range of the S–C–L band as well as nearly zero dispersion at the wavelength of 1.54 μm.

The dispersion slope $S_D(\lambda)$ shown in Fig. 6(a) is an important parameter to describe the property of ultra-flattened dispersion for the proposed PCF. It can be seen from Fig. 6(a) that the optimized PCF presents a nearly zero negative dispersion slope, which will offer the possibility of efficient supercontinuum generation.[23] Figure 6(b) also shows the anti-symmetric relationship of the nonlinearity coefficient γ (λ) and the effective mode area A_{eff} (λ) for the optimized HNDF-PCF. It can be seen from Fig. 6(b) that A_{eff} (λ) is as small as 3.25 μm^2 at the wavelength of 1.55 μm for the optimized HNDF-PCF, which will induce a larger nonlinearity coefficient closed to 46 $\mathrm{W^{-1}\cdot km^{-1}}$. Obviously, the nonlinearity coefficient $\gamma(\lambda)$ of the optimized HNDF-PCF has a sound improvement, which is 4 times larger than that of the commercial high nonlinear PCF, and it will have an important application in the nonlinear four-wave mixing effect.[24]

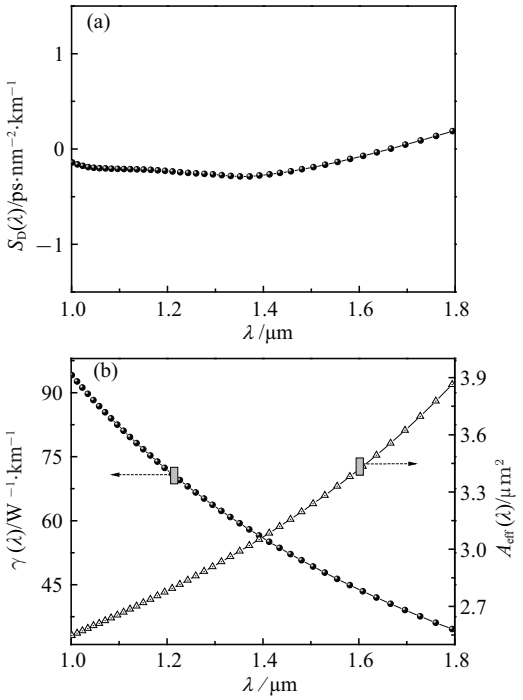


Fig. 6. (a) Dispersion slope versus wavelength; (b) anti-symmetric curves of nonlinearity coefficient γ (λ) and the effective mode area A_{eff} (λ) for the proposed HNDF-PCF with optimized design parameters $\eta = 0.8$, $f = 0.8$, and $\Lambda = 1.6$ μm.

In general, the six-fold symmetry of the PCF guarantees the degeneracy of the fundamental modes. However, birefringence emerges for the optimized HNDF-PCF because of the non-symmetry of its elliptical air holes in the cladding. The birefringence is related to the effective refractive index of fundamental modes n_{eff}, which is expressed as[25]

$$B(\lambda) = \left|\mathrm{Re}(n_{\mathrm{eff}}^{y}(\lambda)) - \mathrm{Re}(n_{\mathrm{eff}}^{x}(\lambda))\right|, \tag{8}$$

where n_{eff}^{y} and n_{eff}^{x} are the effective refractive indices of two orthogonal polarization fundamental modes, respectively. The birefringence as a function of wavelength is presented in Fig. 7(a). It can be seen from Fig. 7(a) that the birefringence increases monotonically with the increase of wavelength. In addition, the modal birefringence is close to 3.2×10^{-3} the low loss communication wavelength of 1.55 μm, which is 2 times larger than that in the reported PM-PCF design.[26,27] The optimized HNDF-PCF with high birefringence can be used in applications in polarization-maintaining communication systems. The confinement leakage loss of the optimized HNDF-PCF is shown in Fig. 7(a). From the results in Fig. 7(a), we

can clearly observe the remarkably low confinement leakage loss for the optimized HNDF-PCF with only seven air-hole-rings, which is 0.016 dB · km^{-1} at the wavelength of 1.55 μm. The confinement loss of the next higher order mode is calculated to be larger than 10 dB · km^{-1} for wavelengths above $\lambda = 1.5$ μm, which ensures the effective single mode operation of this fiber in the telecommunication window.

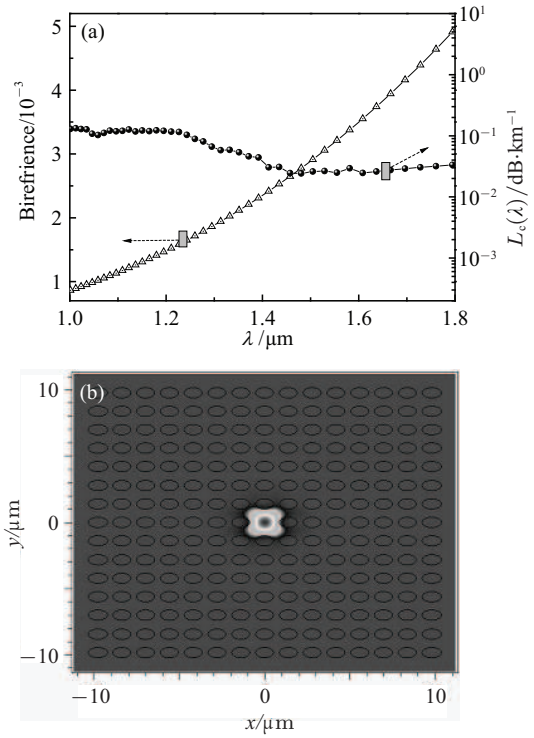


Fig. 7. (a) Birefringence and confinement loss each as a function of wavelength; (b) electric field distribution of the fundamental mode at the wavelength of 1.55 μm for the optimized HNDF-PCF with $\Lambda = 1.6$ μm, $f = 0.8$, and $\eta = 0.8$.

The good mode confinement can also be observed from the normalized electric field distribution of the fundamental mode shown in Fig. 7(b). The stronger mode confinement can give rise to a lower confinement leakage loss.[28] Hence, the proposed HNDF-PCF has a nearly zero ultra-flattened dispersion and a nearly zero negative dispersion slope, and the incorporation of admirable low-loss and low effective mode area together with inducing a high nonlinearity coefficient will have important applications for broadband SC generation, soliton pulse transmission, nonlinear optical loop mirror, wavelength conversion, and so on.

4. Conclusions

In conclusion, a simple controlling technique of chromatic dispersion in index-guiding PCF was applied to propose a HNDF-PCF. A seven-ring HNDF-PCF with low and flat dispersion, low confinement loss, large nonlinear coefficient, and high birefringence has been designed by simply changing the hexangular lattice cladding structure to a square lattice structure and changing the circular cladding air holes to elliptical air holes. The numerical simulations were performed by adopting the full-vector finite element method, and the optimized structure parameters of the proposed PCF were obtained by adjusting its structure parameters, such as the lattice constant Λ, the air-filling fraction f, and the air-hole ellipticity η. The numerical results show that a nearly zero negative dispersion slope is obtained for the optimized PCF with structure parameters of $f = 0.8$, $\eta = 0.8$, and $\Lambda = 1.6$ μm. A chromatic dispersion as low as ±2.5 ps · nm^{-1} · km^{-1} over an ultra-broad waveband range including the S–C–L band, a nearly zero dispersion at the wavelength of 1.54 μm, and a nonlinear coefficient as large as 46 W^{-1} · km^{-1}, a confinement leakage loss as low as 0.016 dB · km^{-1}, and a birefringence as high as 3.2×10^{-3} for the low loss communication wavelength of 1.55 μm have been obtained. The optimized HNDF-PCF is suitable for use in applications such as a chromatic dispersion controller and a dispersion compensator, and can be used in nonlinear optical systems and for efficient super-continuum generation[29] in the telecommunication window.

References

[1] Russell P St J 2003 *Science* **299** 358
[2] Fu B, Li S G, Yao Y Y, Zhang L and Zhang M Y 2011 *Chin. Phys.* B **20** 024209
[3] Gander M J, McBride R, Jones J D C, Mogilevtsev D, Birks T A, Knight J C and Russell P St J 1999 *Electron. Lett.* **35** 63
[4] Ferrando A, Silvestre E, Andrés P, Miret J J and Andrés M V 2001 *Opt. Express* **9** 687
[5] Reeves W H, Knight J C, Russell P St J and Roberts P J 2002 *Opt. Express* **10** 609
[6] Deng Y, Lin Q, Lu F, Agrawal G P and Knox W H 2005 *Opt. Lett.* **30** 1234
[7] Andrei B F, Aleksandr N N, Aleksei M Z, Ignac B, Dusan C Jr, Dusan C, Alexander P T and Dietrich von der L 2002 *J. Opt. Soc. Am.* B **19** 2156
[8] Liu X M, Yang X, Lu F, Ng J, Zhou X and Lu C 2005 *Opt. Express* **13** 142
[9] Liu X M, Zhou X, Tang X, Ng J, Hao J, Chai T Y, Edward L and Lu C 2005 *IEEE Photon. Technol. Lett.* **17** 1626
[10] Dai Y and Shu C 2011 *Opt. Express* **19** 2952
[11] Saitoh K, Koshiba M, Hasegawa T and Sasaoka E 2003 *Opt. Express* **11** 843
[12] Ferrando A, Silvestre E, Miret J J and Andres P 2000 *Opt. Lett.* **25** 790
[13] Wu T L and Chao C H 2005 *IEEE. Photon. Technol. Lett.* **17** 67
[14] Saitoh K and Koshiba M 2004 *Opt. Express* **12** 2027
[15] Zhang Y, Li K, Wang L, Ren L, Zhao W, Miao R, Large M C J and van Eijkelenborg M A 2006 *Opt. Express* **14** 5541
[16] Saitoh K and Koshiba M IEEE 2002 *J. Quantum Elencron.* **38** 927
[17] Koshiba M and Tsuji Y J 2000 *Lightw. Technol.* **18** 737
[18] Zhao X, Zhou G, Li S, Liu Z, Wei D, Hou Z and Hou L 2008 *Appl. Opt.* **47** 5190
[19] Nguyen H C, Kuhlmey B, Steel M J, Smith C, Magi E, McPhedran R C and Eggleton B 2005 *Opt. Lett.* **30** 1123
[20] Poli F, Cucinotta A, Selleri S and Bouk A 2004 *IEEE Photon. Technol. Lett.* 16 1065
[21] Zhang Y N 2011 *Appl. Opt.* **50** E125
[22] Liu X M 2008 *Phys. Rev.* A **77** 043818
[23] Yamamoto T, Kubota H, Kawanishi S, Tanaka M and Yamaguchi S 2003 *Opt. Express* **11** 1537
[24] Biancalana F, Skryabin D V and Russell P St J 2003 *Phys. Rev.* E **68** 046603
[25] Yin G B, Li S G, Wang X Y and Liu S 2011 *Chin. Phys.* B **20** 090701
[26] Zhang Y N 2008 *J. Mod. Opt.* **55** 3563
[27] Zhang Y N, Miao R, Ren L, Wang H, Wang L and Zhao W 2007 *Chin. Phys.* **16** 1719
[28] Finazzi V, Monro T M and Richardson D J 2003 *J. Opt. Soc. Am.* B **20** 1427
[29] Wang X Y, Li S G, Liu S, Yin G B and Li J S 2012 *Chin. Phys.* B **21** 054220